HHS Public Access

Author manuscript

Dev Dyn. Author manuscript; available in PMC 2023 December 15.

Published in final edited form as:

Dev Dyn. 2022 November ; 251(11): 1780–1797. doi:10.1002/dvdy.505.

A clinically-relevant residue of POLR1D is required for *Drosophila* development

Ryan J. Palumbo[*],

Alana E. Belkevich,

Haleigh G. Pascual,

Bruce A. Knutson[*]

Department of Biochemistry and Molecular Biology, SUNY Upstate Medical University, 750 East Adams Street, Syracuse, NY 13210

Abstract

Background.—POLR1D is a subunit of RNA Polymerase I and III (Pol I)/III and dysregulation of Pols are associated with several types of disease, including ribosomopathies. The craniofacial disorder Treacher Collins Syndrome (TCS) is one such disease caused by mutations in subunits of RNA Polymerase I, including POLR1D. Here, we characterized a missense mutation and loss of POLR1D in *Drosophila*.

Results.—We found a *Drosophila* line harboring a mutation in POLR1D (G30R) that reduced rRNA levels, slowed larval growth, and arrested larval development. Remarkably, the G30R substitution is at an orthologous glycine in POLR1D that is mutated in a TCS patient (G52E). We showed that the G52E mutation in human POLR1D, and the comparable substitution (G30E) in *Drosophila* POLR1D, reduce their ability to heterodimerize with POLR1C *in vitro*. We also found that POLR1D is required early in the development of *Drosophila* neural cells. Furthermore, an RNAi screen revealed that POLR1D is also required for development of non-neural *Drosophila* cells, suggesting the possibility of defects in other cell types.

Conclusions.—These results establish a role for POLR1D in *Drosophila* development, and present *Drosophila* as an attractive model to evaluate the molecular defects of TCS mutations in POLR1D.

Keywords

POLR1D; Development; TCS; RNA polymerase I/III; ribosomopathy

1. Introduction

RNA Polymerase I (Pol I) is a multi-subunit complex that is responsible for synthesizing three of the four ribosomal RNAs (rRNAs) in eukaryotes. Mutations in Pol I subunits cause

[*]Co-corresponding authors.

Author contributions

RJP, AEB, and BAK designed this study. RJP, AEB, and HGP performed experiments. RJP and AEB wrote the original draft of the manuscript and designed figures. RJP, AEB, HGP, and BAK reviewed and edited the manuscript and figures.

Treacher Collins Syndrome (TCS)[1], a craniofacial disorder that occurs in approximately 1 in every 50,000 live births[2]. TCS occurs as a result of defects in the proliferation and migration of neural crest cells (NCCs) during embryogenesis. NCC function is required for the formation of facial and auditory structures, which are abnormal in TCS patients[3,4].

TCS is caused predominantly by mutations in *TCOF1*, encoding Treacle; however, mutations in *POLR1D* and *POLR1C* are also implicated in TCS, but are less well understood[2]. POLR1D and POLR1C are evolutionarily conserved and shared subunits of both Pols I and III that form a heterodimer required for Pol I/III assembly and function[5,6]. Our current understanding of the effects of mutations in POLR1D and POLR1C on Pol assembly is limited[7], though they ultimately reduce rRNA synthesis[7,8]. For example, G52E is a mutation in a highly-conserved glycine in POLR1D that was identified in a man with non-familial TCS[2,9]. The molecular mechanism by which G52E causes TCS remains unknown; however, since it is located in in the heterodimerization domain of POLR1D, it is expected to disrupt its interaction with POLR1C, hinder Pol assembly, and impair rRNA expression. Impaired rRNA expression is implicated in the pathology of ribosomopathies, which are characterized by sensitivity of highly-proliferative cell populations to mutations that ultimately reduce translational output[10]. NCCs are particularly sensitive to mutations to Treacle, POLR1D, and POLR1C, which reduce rRNA levels, impede ribosome assembly, and reduce translation. As such, TCS is classified as a ribosomopathy[10,11].

Several model systems, including yeast, zebrafish, and mouse, have been established to study ribosomopathies, including TCS caused by loss of POLR1D function[7,12–17]. While useful, these models suffer several drawbacks. For instance, yeast lacks multi-lineage tissue development and cannot be used to study the developmental phenotypes caused by loss of POLR1D function. Importantly, while zebrafish and mouse are more appropriate models to study POLR1D function in development, those studies have relied on the use of complete deletions of *POLR1D*, which precludes the ability to study the molecular consequences and developmental outcomes of TCS disease variants[2,9]. *Drosophila* is emerging as an excellent model system in which to study ribosomopathies due to the high conservation of ribosome biogenesis factors between flies and humans[18,19] and the availability of reagents to interrogate the function of disease-associated genes. Most importantly, *Drosophila* has a long history as a valuable platform for modeling human disease variants[20–23].

Here, we establish a role for POLR1D in *Drosophila* development. We acquired a fly stock harboring an unknown lesion in *POLR1D*, and found that remarkably, the lesion is a missense mutation (G30R) in the same glycine residue that is mutated in a TCS patient (G52E)[2,9]. Just as G52E yields developmental defects in humans, G30R mutant larvae exhibit reduced growth and are developmentally arrested. Consistent with the role of POLR1D in Pol I and Pol III function, we found that *dPOLR1D1* mutant larvae have reduced levels of rRNAs synthesized by both Pol I and Pol III. We also found that binding of human and *Drosophila* POLR1D proteins to their partner POLR1C subunit is similarly impacted by either the E or R mutations, demonstrating the molecular conservation of the POLR1D/POLR1C interaction. Importantly, tissue-specific RNAi revealed a requirement for POLR1D early in the developing *Drosophila* nervous system, which is similar to the requirement of POLR1D early in human embryonic NCC proliferation, and validates the use

of *Drosophila* as a TCS model. An RNAi screen revealed that POLR1D is also required for tissue development outside of the nervous system, including wings, ovaries, and muscles. Our results establish POLR1D as a protein vital to *Drosophila* development, and suggests that *Drosophila* may serve as an additional model system in which to study developmental and molecular defects of TCS caused by mutated POLR1D.

2. Results

2.1. The *dPOLR1D*^{1} allele is a mutation in a clinically-relevant residue.

We acquired a fly stock that harbored an uncharacterized mutant allele of *Drosophila Polr1D* (hereafter referred to as *dPOLR1D*). We sequenced this allele (*dPOLR1D*^{1}) and identified a guanine to adenine transition in an exon common to all three splice isoforms of *dPOLR1D* (Fig. 1A), resulting in a glycine to arginine substitution (G30) (Fig. 1B, **top**). According to the modENCODE Project[24], the dPOLR1D-PA protein isoform is the most ubiquitous and highly-expressed, and therefore we refer to this mutation with respect to that protein isoform, as G30R. Remarkably, the G30R substitution occurs at a highly-conserved glycine that is mutated in a TCS patient, to glutamic acid (G52E) (Fig. 1B, **bottom**).

2.2. dPOLR1D is required for adult viability.

The *dPOLR1D*^{1} allele was generated as part of a large-scale mutagenesis screen[25]. Placing the *dPOLR1D*^{1} allele *in trans* to a large chromosomal deletion (deficiency; Df) uncovering *dPOLR1D* and 133 additional genes resulted in pre-adult lethality[26,27]. In addition to *dPOLR1D*, the Df uncovered an additional two genes involved in translation, *RpL30* and *mRpL13*[28], which encode ribosomal proteins of the large cytoplasmic and mitochondrial ribosomes, respectively (Fig. 1C, **Dfs** A **and** B). Given the collective role of these three genes in cellular translation, the cumulative cellular stress of *RpL30* and *mRpL13* hemizygosity in a *dPOLR1D*^{1}*/Df* background might have contributed to or even caused pre-adult lethality, instead of lethality being attributable to the *dPOLR1D* mutation alone.

To determine whether the loss of *dPOLR1D* causes the pre-adult lethal phenotype independent of *RpL30, mRpL13*, and other genes in the large Df, we crossed heterozygous *dPOLR1D*^{1}*/+* females with heterozygous males comprising a series of progressively smaller Dfs (Fig. 1C), to see if we could recover adult *dPOLR1D*^{1}*/Df* progeny. No adult *dPOLR1D*^{1}*/Df* progeny were recovered from any cross, including to the smallest Df, Df G (Table 1, Fig. 1C), indicating that dPOLR1D is required for adult viability independent of *RpL30, mRpL13*. For all subsequent experiments we crossed female *dPOLR1D*^{1} heterozygotes with males heterozygous for Df G (Fig. 1C), smallest Df uncovering *dPOLR1D*.

2.3. dPOLR1D is required for larval growth and development.

It was originally reported that *dPOLR1D*^{1}*/Df* larvae were viable despite failing to develop into viable adults. Mutant larvae remained small, about the size of first (L1) or second (L2) instar larvae, long after they should have advanced to later developmental stages[27]. However, this study used a larger Df that removed *RpL30*, *mRpL13*, and other genes, as described above. Therefore, we used our new *dPOLR1D*^{1}*/Df* background to test whether larvae still

arrest in the L1 and L2 stages. We collected wild type (wt) and *dPOLR1D*^{1}*/Df* larvae as they began to hatch, aged them to 24–48, 48–72, and 72–120 h AEL (after egg-laying), and observed larval size. These timepoints represent the L1, L2, and L3 phases of larval development, respectively. As expected, wt larvae grow progressively larger from the L1 to the late L3 stage (Fig. 2A-C); however, *dPOLR1D*^{1}*/Df* larvae grew very little over a 120-h timespan (Fig. 2D-F), remaining at a size approximately that of wt L1 larvae (Fig. 2A). These results demonstrate that defective growth results from the loss of *dPOLR1D* function independent of *RpL30* and *mRpL13*.

Our results suggest that *dPOLR1D*^{1}*/Df* larvae arrest in the L1 stage (Fig. 2F), but it was previously reported that *dPOLR1D*^{1}*/Df* larvae (using a large Df) arrest at the L2 stage[27]. To address this discrepancy, we harvested larval cuticles at timepoints corresponding to the L1, L2, and L3 larval instar stages, and quantified the number of teeth in the mouth hooks, as tooth number reliably indicates each larval instar stage[29]. At each time point, the majority of wt larvae were in the expected larval stages (Fig. 2G-I, M-O). In contrast, *dPOLR1D*^{1}*/Df* larvae showed considerable developmental arrest. At 24–48 h, mutant larvae had L1 mouth hooks as expected (Fig. 2J, M), however, at 48–72 h, almost all mutant larvae still had L1 mouth hooks (Fig. 2K, N), though a few had L2 mouth hooks (Fig. 2K′, N). At 72–120 h, approximately half of the larvae had L1 mouth hooks (Fig. 2L, O), while the other half had L2 mouth hooks (Fig. 2L′, O); no L3 mouth hooks were observed (Fig. 2O). Interestingly, *dPOLR1D*^{1}*/Df* L2 mouth hooks were considerably smaller than those in wt (compared Figs. 2K′, L′ with Fig. 2H), consistent with reduced growth in *dPOLR1D*^{1}*/Df* larvae. These results indicate that the dPOLR1D G30R mutation causes reduced growth and developmental arrest at the L2 larval instar stage.

While unlikely, it is possible that the mutant phenotypes we observe are not due to dysfunctional dPOLR1D protein with the G30R mutation, but to reduced gene dosage, as *dPOLR1D*^{1}*/Df* larvae contain only a single allele of *dPOLR1D*. To rule out this possibility, we measured the levels of *dPOLR1D* mRNA in wt and *dPOLR1D*^{1}*/Df* larvae by qRT-PCR. Using primers that anneal to a region common to both the wild-type and mutant *dPOLR1D* alleles, we found no significant difference in the amount of total *dPOLR1D* mRNA between wt and *dPOLR1D*^{1}*/Df* larvae (P=0.4512, Fig. 3). However, at this stage of development, some or all of the total *dPOLR1D* mRNA in *dPOLR1D*^{1}*/Df* larvae might be maternally-inherited wild-type *dPOLR1D* mRNA. Using a primer specific for the wild-type allele of *dPOLR1D*, we found that *dPOLR1D*^{1}*/Df* larvae did not contain any wild-type (maternal) *dPOLR1D* mRNA (P<.001, Fig. 3). These results indicate that in *dPOLR1D*^{1}*/Df* larvae at the 72–120 h time point, there is complete turnover of maternally-derived wild-type *dPOLR1D* mRNA, and dosage compensation to increase expression of the *dPOLR1D*^{1} allele to levels comparable to expression of the wild-type *dPOLR1D* allele in wt larvae. Therefore, the phenotypes we observe are likely due to defective dPOLR1D protein with the G30R substitution, and not due to a lack of *dPOLR1D*^{1} mRNA. It is also possible that the G30R mutation renders the dPOLR1D^{1} protein unstable.

2.4. dPOLR1D is required for rRNA production.

POLR1D forms a heterodimer with POLR1C that is necessary for Pol I and III assembly[5,6], and loss of POLR1D function reduces rRNA accumulation[7,14]. To determine if the G30R mutation causes reduced rRNA levels in *dPOLR1D^{1}/Df* larvae, we performed RT-qPCR on total RNA extracted from wt and *dPOLR1D^{1}/Df* larvae aged to 72–120 h AEL (a time point at which *dPOLR1D^{1}/Df* larvae only express mutant *dPOLR1D^{1}* mRNA, Fig. 3). As expected for a mutation in a shared Pol I and III subunit, *dPOLR1D^{1}/Df* larvae exhibited a significant decrease in the amount of 18S and 28S rRNA (transcribed by Pol I; P=0.0014 and 0.0444, respectively) and 5S rRNA (transcribed by Pol III; P=0.0432) compared to wt (Fig. 4A). The levels of *Tubulin* mRNA, which is transcribed by Pol II, were not significantly affected (P=0.3613). These results suggest that larval growth reduction and developmental arrest in *dPOLR1D^{1}/Df* larvae are the result of compromised Pol I and III function due to the G30R mutation, leading to reduced expression of rRNAs. It is also formally possible that some or all of the rRNAs we are able to detect in *dPOLR1D^{1}/Df* larvae are from maternally-derived ribosomes (see Discussion).

In *Drosophila*, the loss of rDNA repeats on either the X or Y chromosomes reduces rRNA expression and causes morphological defects in the abdominal tergites of adult flies, referred to as the *bobbed* phenotype[30]. Although *dPOLR1D^{1}/+* flies are viable, we hypothesized that the G30R substitution might be a dominant mutation that decreases rRNA levels during development[31], and phenocopies the *bobbed* mutation in adult flies. Indeed, about 25% of *dPOLR1D^{1}/+* adults exhibited a *bobbed* phenotype, compared to only 0.1% of wt adults (P=0.0087, Fig. 4B). These data suggest that the G30R mutation is a dominant mutation with incomplete penetrance, which reduces rRNA expression, and disrupts tergite development. This is strikingly similar to what is observed in TCS patients: most mutations in *POLR1D* are autosomal dominant[2,9] with incomplete penetrance[32], and lead to structural defects in the craniofacial skeleton[3,4].

2.5. *Drosophila*- and human-specific mutations have different effects on POLR1D/POLR1C heterodimer formation.

Mutation of the conserved glycine in humans causes TCS[2,9], and in *Drosophila*, caused reduced larval growth and developmental arrest (Fig. 2), demonstrating an important and conserved role of this glycine residue in human and *Drosophila* development. We sought to characterize the biochemical consequences of the human (G52E) and *Drosophila* (G30R) mutations in POLR1D (Fig. 1B). When modeled on the crystal structure of human POLR1D (hPOLR1D), the G30 residue in dPOLR1D resides within the domain required for heterodimerization with POLR1C (Fig. 5A). Therefore, we hypothesized that both the G52E and G30R mutations affect POLR1D binding to POLR1C, which could explain the developmental defects these mutations cause in humans and *Drosophila*, respectively.

To determine the effect of these mutations on POLR1D binding to POLR1C, we used a bacterial co-expression system to produce 6xHis-tagged dPOLR1D or hPOLR1D proteins harboring either the human (G to E) or *Drosophila* (G to R) variants, together with the relevant POLR1C protein tagged with 3xFLAG. Co-expression of PORL1D and POLR1C together is critical, as one protein can be insoluble in the absence of the other[7].

Cells co-expressing POLR1D and POLR1C were subjected to precipitation by Ni-affinity purification, and analyzed by SDS-PAGE for the *Drosophila* proteins (Figs. 5B, C) or Western blot for the less well-expressed human proteins (Figs. 5D, E).

Ni-affinity purification of wt *Drosophila* POLR1D pulled down dPOLR1C, as expected (Fig. 5B, lanes 1–4), but the G to E mutant pulled down approximately half as much dPOLR1D (Fig. 5B, lane 7, compare with lane 2; Fig. 5C), suggesting that this substitution interferes with heterodimerization. A similar result was obtained for the human proteins: hPOLR1D pulled down hPOLR1C (Fig. 5D, lanes 1–4), but the G to E mutation reduced this interaction (Fig. 5D, lane 7, compare with lane 2; Fig. 5E). This suggests that the molecular pathology of the G52E mutation in the TCS patient[2,9] is likely reduced dimerization between hPOLR1D and hPOLR1C.

In contrast, we found that the *Drosophila* G to R mutation in both dPOLR1D (Fig. 5B, compare lane 6 with lane 2; Fig. 5C) and hPOLR1D (Fig. 5D, compare lane 6 with lane 1; Fig. 5E) did not affect binding to their respective POLR1C proteins. Therefore, in *Drosophila*, the reduced rRNA levels, reduced growth, and developmental arrest caused by the G30R mutation is not likely due to reduced dPOLR1D/dPOLR1C heterodimerization. Instead, the G30R substitution might affect later steps in Pol I and III assembly[7].

2.6. dPOLR1D is required in pre- and post-mitotic cells of the nervous system for development and adult function.

TCS arises from defects in the proliferation and migration of neural crest cells (NCCs), a highly-proliferative cell population that is sensitive to reduced translation caused by loss of POLR1D function[14]. Therefore, we tested if *Drosophila* neural cells are similarly sensitive to loss of POLR1D function. We employed the GAL4/UAS system[33] to induce RNAi-mediated knockdown of *dPOLR1D*[34] in two different neural cell types, and observed the effect on the timing of three developmental landmarks: (i) the onset of larval “wandering”, (ii) pupariation (pupa formation), and (iii) eclosion from the pupal case. We also determined the effect RNAi had on adult viability and behavior.

First, we used the *wor-GAL4* driver[24,35–37] to induce RNAi in neuroblasts, a pre-mitotic cell type, during the embryonic and larval stages. Knockdown in embryonic and larval neuroblasts did not have an effect on any of the developmental events we scored, including the number of days to the onset of wandering (P=0.2063, Fig. 6A), between wandering and pupariation (P=0.0687, Fig. 6B), and between pupariation and eclosion (P=0.1161, Fig. 6C). Unexpectedly, RNAi in embryonic and larval neuroblasts had a profound adverse effect on adult flies. Adults were viable (P=0.3492, Fig. 6D), but they exhibited extreme locomotor defects (Supplemental Video 1). Most flies became stuck in their food and subsequently died. Flies that did not get stuck were nevertheless unable to remain upright or walk, sporadically moving their limbs in an attempt to move, though mostly remaining completely immobile. These results suggest that loss of dPOLR1D function in neuroblasts during embryonic and/or larval development can have severe consequences in adult flies, a circumstance that is analogous to TCS.

Next, we used the *elav-GAL4* driver[19,24,38] to induce RNAi in all neurons (pan-neuronal), which are post-mitotic cells that derive from neuroblasts. This driver is active not only in embryos and larvae, but also in pupae and adults, and pan-neuronal RNAi yielded both developmental and adult phenotypes. The wandering behavior of L3 larvae was delayed by 1.5 ± 0.1 d in *dPOLR1D* RNAi larvae compared to control (P=0.0094, Fig. 6E); however, the number of days between wandering and pupariation (P=0.4187, Fig. 6F) and pupariation and eclosion (P=0.0795, Fig. 6G) were not significantly delayed, similar to RNAi in embryonic and larval neuroblasts.

Unlike RNAi in embryonic and larval neuroblasts, pan-neuronal knockdown throughout all stages of *Drosophila* development strongly reduced adult viability (Fig. 6H, P<0.0001), with nearly 90% of adults failing to eclose. As with RNAi in neuroblasts, *dPOLR1D* knockdown in neurons also results in locomotor defects (Supplemental Video 2). Of the 10% of viable adults, some exhibited a phenotype similar to *wor > dPOLR1D RNAi* flies, being unable to stand or move and only able to move their limbs in an attempt to become upright (Supplemental Video 2**, top right**); these flies commonly became stuck in their food and died. Other flies were able to remain upright, but were otherwise immobile (Supplemental Video 2**, bottom left**). Curiously, *elav > Polr1D RNAi* flies also have a *held-out wings* phenotype (Fig. 6I). This might be due to defects in indirect flight muscle motoneurons[39,40]. These results identify differences between dPOLR1D function in neurons and neuroblasts, and indicate that dPOLR1D is important for key aspects of developmental timing (larval wandering) and adult viability.

2.7. An RNAi screen reveals a requirement for dPOLR1D function for proper development in a variety of cell types.

Ribosomopathies are thought to be cell type-specific diseases, wherein certain cell populations that have an intrinsically high demand for translation are particularly sensitive to mutations that lead to reduced levels of functional ribosomes[10,41,42]. We were curious as to whether dPOLR1D levels are also important for the development of non-neural cell types. To address this possibility, we took advantage of the wealth of genetic tools available to conduct RNAi screens in *Drosophila* across a broad range of cell types. (Fig. 7). We employed the GAL4/UAS system[33] and crossed control or *UAS-dPOLR1D RNAi* flies [34] with TRiP Toolbox *Drosophila* stocks[43]. The toolbox stocks contain common GAL4 drivers active at different developmental timepoints in different cell types, and an inducible *UAS-Dcr-2* transgene to increase the activity of the dsRNA processing pathway, which increases the strength of siRNA-mediated knockdown and the sensitivity of RNAi screens[34]. We also made use of another GAL4 driver (*ey*^{OK107}) previously used to study ribosomopathies in *Drosophila*[37].

As a proof of principle for the sensitivity of this approach, we repeated RNAi against *dPOLR1D* driven by the *elav-GAL4* driver, but with *Dcr-2* co-induced. This resulted in complete pupal lethality (Fig. 7A), as compared to ~90% pupal lethality without *Dcr-2* (Fig. 6H). Interestingly, dead pupae were often observed to have incomplete head development (Fig. 7A), which is similar to what is observed in the most extreme TCS cases, in which severe underdevelopment of the head and face substantially contribute to prenatal

inviability[44,45]. The increased severity of *elav > dPOLR1D RNAi* phenotypes caused by co-induction of *Dcr-2* demonstrated the sensitivity of this approach, and ensured that we would detect developmental defects caused *dPOLR1D* knockdown in other tissues.

We found that *dPOLR1D* RNAi induced in a range of cell types caused various developmental or functional defects, indicating a broad and temporal requirement for dPOLR1D function in development (Fig. 7). *en-GAL4* is expressed in the posterior compartment of larval imaginal discs[46] as well as the central nervous system (CNS)[47,48]. *dPOLR1D* knockdown induced by *en-GAL4* inhibited the eversion of the anterior spiracles (Fig. 7B, red arrowheads) and resulted in complete pupal lethality. Anterior spiracles are required for pupal respiration, and failure to evert likely accounts for the complete pupal lethality we observe. Induction of *dPOLR1D* knockdown in the eye discs with the ey^{OK107} GAL4 driver[49] caused a mild “rough eye” phenotype (Fig. 7C, white arrowhead), suggesting that reduced dPOLR1D function can cause cell death in the eye[50]. Cell death due to loss of POLR1D function therefore appears to be a conserved cellular response across multiple model organisms[14,17,51]. *bbg-GAL4* is expressed in the dorsoventral boundary of the wing discs[52], and *Bx-GAL4* is expressed in the wing hinge and wing pouch regions of the wing disc[53]. *dPOLR1D* knockdown induced by these GAL4 drivers led to *scalloped* wing (Fig. 7D, red arrowhead) and *vestigial* wing (Fig. 7E, red arrowhead) phenotypes. Scalloped has a function in both Hippo and Wingless signaling[54,55], and interacts physically with Vestigial[56], suggesting that dPOLR1D may function in the Scalloped/Vestigial axis. Like *Bx-GAL4*, *nub-GAL4* is also expressed in the wing hinge and wing pouch of the wing discs[57]; however, unlike RNAi induced with *Bx-GAL4*, induction with *nub-GAL4* led to complete truncation of the wings at the wing hinge (Fig. 7F). This difference may be due to the exact timing or location of *nub-GAL4* expression compared to *Bx-GAL4*. *dPOLR1D* knockdown induced in the female germline with *nos-GAL4.NGT*[58] strongly reduced ovary size (Fig. 7G, **top**), and rendered females sterile ($P<0.0001$, Fig. 7G, **bottom**). This is consistent with the high demand for Pol I transcription factors in female germline[59,60]. *dPOLR1D* knockdown in muscles with *Mef2-GAL4*[61] caused a reduction in larval growth and arrested larval development (Figs. 7H, I), phenocopying the developmental arrest of $dPOLR1D^{1}/Df$ larvae (Fig. 2E-H).

In summary, the results of our RNAi screen suggest that dPOLR1D functions in the development of a broad range of cell types, and serves as a resource for future investigations into the developmental role of dPOLR1D in a variety of cells, tissues, and organs.

3. Discussion

Here, we established *Drosophila* as a tractable model for studying both the role of POLR1D (and other Pol I/III subunits) in organismal development, and TCS (Fig. 8). We show that a G to R substitution in a conserved glycine in the *Drosophila* ortholog of POLR1D reduces rRNA levels and larval growth, and arrests larval development (Fig. 8A). Introducing a TCS patient mutation (G to E) at this position reduced the ability of the *Drosophila* and human POLR1D to heterodimerize with POLR1C *in vitro*. Importantly, we show that RNAi-mediated knockdown of *dPOLR1D* in pre- and post-mitotic neural cells reduces developmental rate and adult viability, and affects the ability of viable adults to functional

normally, which is similar to the effect POLR1D mutants have on TCS patients (Figs. 8C, F). Finally, an RNAi screen demonstrated that dPOLR1D has a role in the development and function of non-neural cell types, including the muscles (Fig. 8B), imaginal discs (Fig. 8C), wings (Fig. 8D), and ovaries (Fig. 8E).

We discovered that a classic *dPOLR1D* mutant fly line[25] harbors an amino acid substitution (G30R) of a glycine residue that corresponds to a glycine (G52E) in human POLR1D that is mutated in a patient with non-familial TCS[2,9]. In our experiments, the human mutation (G to E) in both *Drosophila* and human POLR1D proteins reduced, but did not abolish binding to their cognate POLR1C proteins. This is not surprising, however, given that most protein-protein interactions require multiple contacts. The fact that a single amino acid replacement within a larger dimerization domain significantly disrupted the POLR1D/POLR1C interaction strongly suggests that in patients with a G52E mutation, TCS is caused by reduced heterodimer formation.

Although the *Drosophila* mutation (G to R) did not affect heterodimer formation *in vitro*, it did reduce the levels of the 18S, 28S, and 5S rRNAs in $dPOLR1D^{1}/Df$ larvae. We suspect that G30R might inhibit Pol I and III assembly downstream of heterodimerization, leading to impaired rRNA synthesis. In support of this idea, a TCS mutation at a conserved threonine (T71I) in AC19, the yeast ortholog of POLR1D, blocks Pol I and III assembly downstream of heterodimerization, leading to impaired rRNA synthesis[7]. The conserved threonine is within the heterodimerization domain, two positions away from the conserved glycine.

Interestingly, mutation of the glycine to two different amino acids resulted in two distinct biochemical phenotypes that reflect the major function of POLR1D in heterodimer formation and Pol I/III assembly. This indicates that the identity of an amino acid substitution at a given position can dramatically influence the corresponding biochemical phenotype. The opposing effects of the E and R mutations on the POLR1D/POLR1C interaction might be due to their opposing charges; however, the demonstration that either mutation had the same effect on both *Drosophila* and human POLR1D (i.e. disrupted or undisrupted binding to POLR1C) underscores the molecular conservation of the POLR1D/POLR1C interaction. Most importantly, our results suggest that this conserved glycine is important for both heterodimerization with POLR1C and Pol I/III assembly, and is vital to both *Drosophila* and human development.

Based on our results that showed the G30R mutation caused reduced levels of zygotic rRNA and arrested larval development at the L2 stage, it appears that maternally-deposited rRNAs and ribosomes are sufficient to sustain larval development to L2, but not sufficient to support the massive growth required to progress to the L3 stage. dPOLR1D function is therefore required to provide an ample supply of rRNAs to enable developmental progression. This is strikingly similar to what occurs in *Drosophila* larvae harboring a *Nopp140* deletion, which reduces accumulation of mature, 2′-O-methylated 18S and 28S rRNAs, coincident with reduced larval growth, and arrest in the L2 stage[62]. Similarly, in *C. elegans* larvae that are deleted of all rDNA repeats (and thus contain only maternally-derived ribosomes), development stalls at the L1 larval stage[63]. Therefore, it appears that there is a certain

threshold of mature rRNAs that is required at different stages of larval development in metazoans to allow for growth to occur, and development to proceed.

TCS is a disease that predominantly affects the NCCs, wherein mutations in *POLR1D* and other Pol I/III pathway genes prevent cell proliferation and migration, cause cell death, and lead to craniofacial defects[3,8,10,14,64]. While *Drosophila* lack NCCs per se, we nevertheless found that RNAi knockdown of *dPOLR1D* in *Drosophila* neural cells yields adverse effects that are analogous to those in TCS patients with POLR1D mutations. Knockdown of *dPOLR1D* in embryonic and larval neuroblasts, and neurons, severely compromised the locomotor abilities of adult flies. Therefore, typical adult locomotor behavior requires dPOLR1D function in neural cells during the preceding embryonic and larval stages, which is analogous to TCS caused by mutations in *POLR1D*, where normal fetal development is compromised by a lack of POLR1D function in NCCs during embryogenesis[44,45]. Additionally, pan-neuronal knockdown throughout all stages of development severely reduced adult viability, with almost all flies dying as pupae. Pupal lethality is similar to what is observed in TCS patients with the most severe craniofacial defects, where prenatal and postnatal survival is reduced due to severely underdeveloped facial structures and an inability to properly breathe or feed[44,45]. Overall, our findings establish a parallel between the requirement of POLR1D in *Drosophila* and human neural cells, for larval and embryonic development, respectively. It will be interesting to determine the exact mechanism by which the G30R mutation and disease variants found in human POLR1D act in neuroblasts and neurons to cause developmental arrest in the *Drosophila* model.

Our RNAi screen revealed that, in addition to neural cells, many cell types are sensitive to *dPOLR1D* knockdown. We speculate that this is likely the case in humans too. RNAi represents an extreme condition of POLR1D loss-of-function that does not underly most cases of TCS caused by POLR1D mutations, which are typically autosomal dominant and hypomorphic[2,9,65,66]. However, some TCS patients have been identified that are homozygous for a recessive allele of *POLR1D*[67]. It remains possible that lethal cases of TCS are caused by homozygosity for strong mutant alleles of *POLR1D* that affect not only NCCs, but other cells types required for embryonic viability that are otherwise resistant to heterozygosity for dominant *POLR1D* mutations; this circumstance would most closely reflect the results of our RNAi screen. Our screen also lays the groundwork for future studies to address the function of dPOLR1D in additional tissues and at different developmental stages, both by RNAi, and by the construction of transgenic fly lines possessing POLR1D mutations found in TCS patients. Taken together, our results demonstrate that *Drosophila* is an attractive model in which to study the molecular and developmental consequences of TCS mutations in POLR1D.

4. Experimental Procedures

4.1. Fly stocks and husbandry

Flies were raised on Nutri-Fly MF food (Genesee Scientific) with ~0.064 M propionic acid (Sigma Aldrich, P5561), at 18–25ºC and 50–80% humidity, on a 12 h light/dark cycle. RNAi experiments were carried out at 29–30ºC.

Polr1D^{1} *pr*^{1}*/CyO* (referred to in the text as *dPOLR1D*^{1}*/CyO*; BDSC #3304) was rebalanced by outcrossing to *wg*$^{Sp-1}$*/CyO* (BDSC #259) and inbreeding *Curly* F1 progeny lacking the dominant *wg*$^{Sp-1}$ allele. The rebalanced *dPOLR1D*^{1}*/CyO* stock and *Exel8040/CyO* (a deficiency uncovering *dPOLR1D;* BDSC #7847) were rebalanced by outcrossing to *Sco*^{rv9R}*/CyO, ActGFP* (BDSC #4533), a stock ubiquitously expressing GFP from a *CyO* balancer chromosome. GFP-expressing progeny lacking the dominant *Sco*^{rv9R} allele were inbred to generate *dPOLR1D*^{1}*/CyO, ActGFP* and *Exel8040/CyO, ActGFP* stocks. When these two lines are crossed, *dPOLR1D*^{1}*/Df* larval progeny are identifiable by the absence of GFP.

Oregon-R-P2 (BDSC #2376) was wt for all *dPOLR1D*^{1}*/Df* experiments. *w; BSC341/CyO* (BDSC #24365) is a deficiency uncovering *dPOLR1D. w; Exel6042/CyO* (BDSC #7524), *w; ED1200/SM6a* (BDSC #9173), and *w; ED1226/SM6a* (BDSC #9288) are deficiencies uncovering *dPOLR1D* and *RpL30. w; ED1202/SM6a* (BDSC #24466) and *w; ED1203/SM6a* (BDSC #8935) are deficiencies uncovering *dPOLR1D*, *RpL30, and mRpL13. yw; VIE-260B* (VDRC #60100) was the control for RNAi experiments. *yw; P{KK108376}VIE-260B* (VDRC #100595) harbors a GAL4-inducible dsRNA targeting *dPOLR1D*. GAL4 lines used in this study are: *UAS-Dcr-2, w; bbg-GAL4* (BDSC #25757), *w Bx-GAL4; UAS-Dcr-2* (BDSC #25706), *elav-GAL4* (BDSC #458), *elav-GAL4 w; UAS-Dcr-2* (BDSC #25750), *UAS-Dcr-2, w; en-GAL4, UAS-2xEGFP* (BDSC #25752), *w; ey*^{OK107} (BDSC #854), *UAS-Dcr-2, w; Mef2-GAL4* (BDSC #25756), *UAS-Dcr-2, w; nosGAL4.NGT* (BDSC #25751), *UAS-Dcr-2, w; nub-GAL4* (BDSC #25754), and *w; wor-GAL4; Dr*^{1}*/TM3, Ubx-lacZ*, Sb^{1} (BDSC #56553).

4.2. Crosses to assess *dPOLR1D*^{1}*/Df* adult viability

Heterozygous *dPOLR1D*^{1}*/CyO* females were crossed with wt, heterozygous *Df/CyO,* or heterozygous *Df/SM6a* males. In crosses with heterozygotes, the wt allele of *dPOLR1D* is provided by either *CyO or SM6a*, which are recessive lethal chromosomes with a dominant negative allele causing a *Curly* wing phenotype. Thus, adult *dPOLR1D*^{1}*/Df* progeny are identifiable by the absence of *Curly* wings.

4.3. Egg collections and larvae isolation

Females and males were crossed at a 3:1 ratio in cages, and eggs were collected every 2–4 h on grape juice agar (Genesee Scientific) plates with yeast paste. Larvae were hand-selected 24–48 h AEL, and transferred to fresh grape juice agar plates with yeast paste. Larvae were aged to the appropriate time point, and either imaged, or flash-frozen in liquid nitrogen or a dry ice/ethanol bath, and stored at −80ºC.

4.4. Larval cuticle preparations and imaging

Larvae frozen at −80ºC were thawed and mounted on slides with a solution of 3:1 lactic acid:sterile water, covered with a coverslip, and incubated overnight at 60ºC. The anteriors of L3 larvae that were cut in half were mounted to facilitate easier mounting. Slides were sealed with nail polish, and scored and imaged under DIC optics.

4.5. Nucleic acid purification

Genomic DNA was purified from 10 adult male flies with the Monarch Genomic DNA Purification Kit (New England Biolabs, Inc) according to the manufacturer's instructions. Total RNA was purified from either 4 wt or ~300 *dPOLR1D*^{1}*/Df* larvae collected at 72–120 h AEL, with the Monarch Total RNA Purification Kit (New England BioLabs, Inc) according to the manufacturer's instructions for preparation of total RNA from tissues.

PCR and sequencing of adult flies—PCR was performed on gDNA from wt or *dPOLR1D*^{1}*/CyO* males using OneTaq Hot Start 2X Master Mix with Standard Buffer (New England Biolabs, Inc) with primers *dPOLR1D-F* (5′-AAT GGA AGA GGA ACG CAG CC-3′) and *dPOLR1D-R* (5′-AAC TAC GAT CCC AAG AAG GC-3′). PCR products were sequenced by Molecular Cloning Laboratories, with either *dPOLR1D_Seq_1* (5′-TAG TTG AGC CTC TGA ACT GG-3′) or *dPOLR1D_Seq_2* (5′-CAT CGA TGA CGT TAC CAC GG-3′).

4.6. RT-qPCR

RT-qPCR was performed on 10 pg (rRNA targets) or 1–100 ng (other targets) of total RNA with the Luna Universal One-Step RT-qPCR Kit (New England BioLabs, Inc) according to the manufacturer's instructions. Reactions were performed in biological quadruplicate and technical triplicate, using a CFX Opus 384 (Bio-Rad) and the data were analyzed using Bio-Rad Maestro software. The wild type allele of *dPOLR1D* was amplified using the ARMS approach [68,69], with primers *Wild_Type_dPOLR1D-F* (5′-CAA CGA GGG CCA CAC GCT TG-3′), and *dPOLR1D_RT-R* (5′-TAT GAT CAC ACA GAC CCT CC-3′). Total *dPOLR1D* mRNA (i.e. the wild type and mutant alleles of *dPOLR1D* were amplified with *Total_dPOLR1D-F*, a primer common to both alleles (5′-TTT GTG TTC ACC AAC GAG GG-3′), and *dPOLR1D_RT-R.* The primers used to amplify the 18S and 28S rRNAs [31], and 5S rRNA [70], were described previously. The primers used to amplify α*Tub84B* (*Tubulin*) were α*Tub84B-F* (5′-AGC GTC ACG CCA CTT CAA CG-3′) and α*Tub84B-R* (5′-CTG ACA ACA CTG AAT CTG GC-3′). *Act5C (Actin*) was used as the reference gene in all experiments, and was amplified with primers *Act5C-F* (5′-GAT GGT CTT GAT TCT GCT GG-3′) and *Act5C-R* (5′-CTG GAA CCA CAC AAC ATG CG-3′).

4.7. Structural Modeling of dPOLR1D

dPOLR1D was modeled onto hPOLR1D (PDB 7AE1, chain K) using the HHpred MPI Bioinformatics Toolkit using default settings[71,72].

4.8. Heterodimer Co-expression Assay and Analysis

POLR1D and POLR1C orthologs were cloned into coexpression compatible pET-DUET-1 (Novagen, 71146) and pCDF-DUET-1 (Novagen, 71340), respectively. The sequences used were NM_136106 for *dPOLR1D*, NM_135041 for *dPOLR1C*, NM_001374407.1 for *hPOLR1D*, and NM_203290.4 for *hPOLR1C*. Mutations in *POLR1D* were made using Quikchange mutagenesis[73] with the following primers: *dPOLR1D_G30R_F* (5′-CAC ACG CTG AGA AAT GCG CTG AAA ACG ATC ATA-3'), *dPOLR1D_G30R_R* (5′-CAG CGC ATT TCT CAG CGT GTG GCC CTC GTT GGT-3′), *dPOLR1D_G30E_F* (5′-CAC

ACG CTG GAG AAT GCG CTG AAA ACG ATC ATA-3′), *dPOLR1D_G30E_R* (5′-CAG CGC ATT CTC CAG CGT GTG GCC CTC GTT GGT-3′), *hPOLR1D_G52R_F* (5′-CAT ACC CTA CGT AAT TCT CTA CGT TAC ATG ATC-3′), *hPOLR1D_G52R_R* (5′-TAG AGA ATT ACG TAG GGT ATG GTC TTC CTC GTG-3′), *hPOLR1D_G52E_F* (5′-CAT ACC CTA GAG AAT TCT CTA CGT TAC ATG ATC-3′), *hPOLR1D_G52E_R* (5′-TAG AGA ATT CTC TAG GGT ATG GTC TTC CTC GTG-3′). Complexes of recombinant wt or mutant dPOLR1D or hPOLR1D, with dPOLR1C and hPOLR1C, were expressed in BL21(DE3) Rosetta2 pLysS cells in Auto-inducing Terrific Broth (0.024% w/v tryptone, 0.048% yeast extract w/v, 0.4% v/v glycerol, 17 mM KH_2PO_4, and 72 mM K_2HPO_4) supplemented with 5052 solution (0.5% glycerol, 0.05% glucose, and 0.2% alpha lactose monohydrate) and 2mM $MgSO_4$ for18 hours at 37°C. Cells were harvested by centrifugation, washed with extract buffer (20mM Tris-HCl ph 7.5, 200 mM KCl, 10% Glycerol, 0.1 mM EDTA, 20 mM Imidazole, 0.05% Tergitol), and lysed by sonication. The solution was then cleared and added to Ni-NTA affinity beads (GE Healthcare) and incubated at 4°C for 18 hours. Complex-bound beads were washed four times with wash buffer (20mM Tris-HCl ph 7.5, 750 mM KCl, 10% Glycerol, 0.1 mM EDTA, 20 mM Imidazole, 0.05% Tergitol) and eluted with elution buffer (20mM Tris-HCl ph 7.5, 200 mM KCl, 10% Glycerol, 0.1 mM EDTA, 250 mM Imidazole, 0.05% Tergitol). Elutions were pooled and analyzed by SDS-PAGE and Coomassie Blue stain or Western Blot. Primary antibodies used were His Tag Antibody (1:2000, AVIVA, OAEA00010) and Anti-FLAG M2 (1:2000, Sigma, F1804). Blots were incubated in goat anti-Mouse IRDye680 (1:10,000, LiCor, 926–68070) secondary antibody and imaged using the Odyssey FC (LiCor) imager. Densitometry was performed using Fiji (version 2.3.0/1.53f). Mutant POLR1D pulldowns were made relative to the wild-type POLR1D pulldown that had a similar POLR1D band intensity.

4.9. Scoring Neural Cell RNAi

Two *wor-GAL4* or *elav-GAL4* virgin females were crossed with two control or *dPOLR1D* RNAi males in vials with active yeast pellets at 29ºC. Crosses were performed in biological triplicate, flipped every 24 h for 3 d for a total of three technical replicates. The state of each culture was observed daily to determine the number of days between: egg-laying and larval wandering behavior, wandering and pupariation, and pupariation and eclosion. Adult viability was determined by counting the total number of pupae and adults that hatched from them.

4.10. Fertility Assay

Virgin females were crossed to wt males in vials for 2–3 days. At 4 days post-eclosion, females and 2–3 males were split into individual vials with dry active yeast to promote oogenesis. At 5 days post-eclosion, crosses were flipped into fresh vials, and females were allowed to lay eggs for 24 h prior to counting the number of eggs laid per female per day. Crosses were performed in biological triplicate.

Supplementary Material

Refer to Web version on PubMed Central for supplementary material.

Acknowledgements

The authors thank N. Alic, P. DiMario and S. Neal for helpful discussions about experimental methods; E. Leathermann (Hanes Lab) for technical assistance; members of the Knutson Lab, S. Neal, and S. Hanes for comments on the manuscript; and the Bloomington and Vienna *Drosophila* Stock Centers for fly lines. This work was supported by grants awarded to BAK (NIH R03-DE027785, NIH R01-GM141033). RJP was supported in part by a grant awarded to S. Hanes (NIH R01-GM123985).

References

1. Sharifi S, Bierhoff H. Regulation of RNA Polymerase I Transcription in Development, Disease, and Aging. Annual Review of Biochemistry. 2018–06-20 2018;87(1):51–73. 10.1146/annurev-biochem-062917-012612.
2. Dauwerse JG, Dixon J, Seland S, et al. Mutations in genes encoding subunits of RNA polymerases I and III cause Treacher Collins syndrome. Nat Genet. Jan 2011;43(1):20–2. 10.1038/ng.724. [PubMed: 21131976]
3. Trainor PA. Craniofacial birth defects: The role of neural crest cells in the etiology and pathogenesis of Treacher Collins syndrome and the potential for prevention. Am J Med Genet A. Dec 2010;152A(12):2984–94. 10.1002/ajmg.a.33454. [PubMed: 20734335]
4. Serrano F, Bernard WG, Granata A, et al. A Novel Human Pluripotent Stem Cell-Derived Neural Crest Model of Treacher Collins Syndrome Shows Defects in Cell Death and Migration. Stem Cells Dev. Jan 15 2019;28(2):81–100. 10.1089/scd.2017.0234. [PubMed: 30375284]
5. Werner F, Grohmann D. Evolution of multisubunit RNA polymerases in the three domains of life. Nat Rev Microbiol. Feb 2011;9(2):85–98. 10.1038/nrmicro2507. [PubMed: 21233849]
6. Wild T, Cramer P. Biogenesis of multisubunit RNA polymerases. Trends Biochem Sci. Mar 2012;37(3):99–105. 10.1016/j.tibs.2011.12.001. [PubMed: 22260999]
7. Walker-Kopp N, Jackobel AJ, Pannafino GN, Morocho PA, Xu X, Knutson BA. Treacher Collins syndrome mutations in Saccharomyces cerevisiae destabilize RNA polymerase I and III complex integrity. Hum Mol Genet. Nov 1 2017;26(21):4290–4300. 10.1093/hmg/ddx317. [PubMed: 28973381]
8. Terrazas K, Dixon J, Trainor PA, Dixon MJ. Rare syndromes of the head and face: mandibulofacial and acrofacial dysostoses. Wiley Interdiscip Rev Dev Biol. May 2017;6(3). 10.1002/wdev.263.
9. Vincent M, Genevieve D, Ostertag A, et al. Treacher Collins syndrome: a clinical and molecular study based on a large series of patients. Genet Med. Jan 2016;18(1):49–56. 10.1038/gim.2015.29. [PubMed: 25790162]
10. Yelick PC, Trainor PA. Ribosomopathies: Global process, tissue specific defects. Rare Dis. 2015;3(1):e1025185. 10.1080/21675511.2015.1025185.
11. Danilova N, Gazda HT. Ribosomopathies: how a common root can cause a tree of pathologies. Dis Model Mech. 2015;8(9):1013–1026. 10.1242/dmm.020529. [PubMed: 26398160]
12. Jones NC, Lynn ML, Gaudenz K, et al. Prevention of the neurocristopathy Treacher Collins syndrome through inhibition of p53 function. Nat Med. 2008;14(2):125–133. 10.1038/nm1725. [PubMed: 18246078]
13. Achilleos A, Watt K, Trainor P. Genetic dissection of Treacher Collins Syndrome: Polr1c and Polr1d. Faseb J. 2013;27(S1). 10.1096/fasebj.27.1_supplement.21.3.
14. Noack Watt KE, Achilleos A, Neben CL, Merrill AE, Trainor PA. The Roles of RNA Polymerase I and III Subunits Polr1c and Polr1d in Craniofacial Development and in Zebrafish Models of Treacher Collins Syndrome. Plos Genet. Jul 2016;12(7):e1006187. 10.1371/journal.pgen.1006187.
15. Sakai D, Dixon J, Achilleos A, Dixon M, Trainor PA. Prevention of Treacher Collins syndrome craniofacial anomalies in mouse models via maternal antioxidant supplementation. Nat Commun. Jan 21 2016;7(1):10328. 10.1038/ncomms10328. [PubMed: 26792133]
16. Tse WK. Treacher Collins syndrome: New insights from animal models. Int J Biochem Cell Biol. Dec 2016;81(Pt A):44–47. 10.1016/j.biocel.2016.10.016.

17. Miao X, Sun T, Golan M, Mager J, Cui W. Loss of POLR1D results in embryonic lethality prior to blastocyst formation in mice. Mol Reprod Dev. Nov 2020;87(11):1152–1158. 10.1002/mrd.23427. [PubMed: 33022126]
18. Calamita P, Gatti G, Miluzio A, Scagliola A, Biffo S. Translating the Game: Ribosomes as Active Players. Front Genet. 2018;9(November):533. 10.3389/fgene.2018.00533. [PubMed: 30498507]
19. Takai A, Chiyonobu T, Ueoka I, et al. A novel Drosophila model for neurodevelopmental disorders associated with Shwachman-Diamond syndrome. Neurosci Lett. Nov 20 2020;739(September):135449. 10.1016/j.neulet.2020.135449.
20. Chen KF, Crowther DC. Functional genomics in Drosophila models of human disease. Brief Funct Genomics. Sep 2012;11(5):405–15. 10.1093/bfgp/els038. [PubMed: 22914042]
21. Chow CY, Reiter LT. Etiology of Human Genetic Disease on the Fly. Trends Genet. Jun 2017;33(6):391–398. 10.1016/j.tig.2017.03.007. [PubMed: 28420493]
22. Oriel C, Lasko P. Recent Developments in Using Drosophila as a Model for Human Genetic Disease. Int J Mol Sci. Jul 13 2018;19(7). 10.3390/ijms19072041. [PubMed: 30577572]
23. Baldridge D, Wangler MF, Bowman AN, et al. Model organisms contribute to diagnosis and discovery in the undiagnosed diseases network: current state and a future vision. Orphanet J Rare Dis. May 7 2021;16(1):206. 10.1186/s13023-021-01839-9. [PubMed: 33962631]
24. Celniker SE, Dillon LA, Gerstein MB, et al. Unlocking the secrets of the genome. Nature. Jun 18 2009;459(7249):927–30. 10.1038/459927a. [PubMed: 19536255]
25. Pentz ES, Black BC, Wright TRF. A diphenol oxidase gene is part of a cluster of genes involved in catecholamine metabolism and sclerotization in Drosophila. I. Identification of the biochemical defect in Dox-A2 [l(2)37Bf] mutants. Genetics. 1986;112(4):823–841. 10.1093/genetics/112.4.823. [PubMed: 3082714]
26. Wright TR, Hodgetts RB, Sherald AF. The genetics of dopa decarboxylase in Drosophila melanogaster. I. Isolation and characterization of deficiencies that delete the dopa-decarboxylase-dosage-sensitive region and the alpha-methyl-dopa-hypersensitive locus. Genetics. Oct 1976;84(2):267–85. 10.1093/genetics/84.2.267. [PubMed: 826447]
27. Wright TR. The Wilhelmine E. Key 1992 Invitational lecture. Phenotypic analysis of the Dopa decarboxylase gene cluster mutants in Drosophila melanogaster. J Hered. May-Jun 1996;87(3):175–90. 10.1093/oxfordjournals.jhered.a022983. [PubMed: 8683095]
28. Marygold SJ, Roote J, Reuter G, et al. The ribosomal protein genes and Minute loci of Drosophila melanogaster. Genome Biol. 2007;8(10):R216. 10.1186/gb-2007-8-10-r216. [PubMed: 17927810]
29. Bodenstein D. The postembryonic development of Drosophila. In: Demerec M, ed. Biology of Drosophila. New York: Wiley; 1950:275–367.
30. Ritossa FM, Atwood KC, Spiegelman S. A MOLECULAR EXPLANATION OF THE BOBBED MUTANTS OF DROSOPHILA AS PARTIAL DEFICIENCIES OF “RIBOSOMAL” DNA. Genetics. 1966;54(3):819–834. 10.1093/genetics/54.3.819. [PubMed: 5970623]
31. Corrales GM, Filer D, Wenz KC, et al. Partial Inhibition of RNA Polymerase I Promotes Animal Health and Longevity. Cell Reports. 2020;30(6):1661–1669.e4. 10.1016/j.celrep.2020.01.017. [PubMed: 32049000]
32. Collins ET. Case with symmetrical congenital notches in the outer part of each lower lid and defective development of the malar bones. Trans Ophthalmol Soc UK. 1900;20:191–192.
33. Brand AH, Perrimon N. Targeted gene expression as a means of altering cell fates and generating dominant phenotypes. Development. 1993;118(2):401–415. 10.1242/dev.118.2.401. [PubMed: 8223268]
34. Dietzl G, Chen D, Schnorrer F, et al. A genome-wide transgenic RNAi library for conditional gene inactivation in Drosophila. Nature. Jul 12 2007;448(7150):151–6. 10.1038/nature05954. [PubMed: 17625558]
35. Albertson R, Chabu C, Sheehan A, Doe CQ. Scribble protein domain mapping reveals a multistep localization mechanism and domains necessary for establishing cortical polarity. J Cell Sci. Dec 1 2004;117(Pt 25):6061–70. 10.1242/jcs.01525.
36. Zhu CC, Boone JQ, Jensen PA, et al. Drosophila Activin-β and the Activin-like product Dawdle function redundantly to regulate proliferation in the larval brain. Development. 2008;135(3):513–521. 10.1242/dev.010876. [PubMed: 18171686]

37. Baral SS, Lieux ME, DiMario PJ. Nucleolar stress in Drosophila neuroblasts, a model for human ribosomopathies. Biol Open. Apr 13 2020;9(4):1–14. 10.1242/bio.046565.
38. Lin DM, Goodman CS. Ectopic and increased expression of Fasciclin II alters motoneuron growth cone guidance. Neuron. Sep 1994;13(3):507–23. 10.1016/0896-6273(94)90022-1. [PubMed: 7917288]
39. Crossley AC. The morphology and development of the Drosophila muscular system. The Genetics and Biology of Drosophila. Vol 2. New York: Academic Press; 1978:499–560.
40. Lam G, Hall BL, Bender M, Thummel CS. DHR3 Is Required for the Prepupal–Pupal Transition and Differentiation of Adult Structures during Drosophila Metamorphosis. Dev Biol. 1999;212(1):204–216. 10.1006/dbio.1999.9343. [PubMed: 10419696]
41. Calo E, Gu B, Bowen ME, et al. Tissue-selective effects of nucleolar stress and rDNA damage in developmental disorders. Nature. Feb 1 2018;554(7690):112–117. 10.1038/nature25449. [PubMed: 29364875]
42. Farley-Barnes KO, Lisa; Baserga, Susan. Ribsomopathies: old concepts, new controversies. Trends Genetics. 2019;35(10):754–767.
43. Perkins LA, Holderbaum L, Tao R, et al. The Transgenic RNAi Project at Harvard Medical School: Resources and Validation. Genetics. Nov 2015;201(3):843–52. 10.1534/genetics.115.180208. [PubMed: 26320097]
44. Behrents RG, McNamara JA, Avery JK. Prenatal mandibulofacial dysostosis (Treacher Collins syndrome). Cleft Palate J. Jan 1977;14(1):13–34. [PubMed: 264276]
45. Edwards SF A; Cust MP; Liu DT; Young ID; Dixon, MJ. Prenatal diagnosis in Treacher Collins syndrome using combined linkage analysis and ultrasound imaging. Journal of Medical Genetics. 1996;33:603–606. [PubMed: 8818950]
46. Bejarano F, Gonzalez I, Vidal M, Busturia A. The Drosophila RYBP gene functions as a Polycomb-dependent transcriptional repressor. Mech Dev. Oct 2005;122(10):1118–29. 10.1016/j.mod.2005.06.001. [PubMed: 16125914]
47. Kumar A, Fung S, Lichtneckert R, Reichert H, Hartenstein V. Arborization pattern of engrailed-positive neural lineages reveal neuromere boundaries in the Drosophila brain neuropil. J Comp Neurol. Nov 1 2009;517(1):87–104. 10.1002/cne.22112. [PubMed: 19711412]
48. Shaw RE, Kottler B, Ludlow ZN, et al. In vivo expansion of functionally integrated GABAergic interneurons by targeted increase in neural progenitors. Embo J. Jul 2 2018;37(13). 10.15252/embj.201798163.
49. Chen CC, Wu JK, Lin HW, et al. Visualizing long-term memory formation in two neurons of the Drosophila brain. Science. Feb 10 2012;335(6069):678–85. 10.1126/science.1212735. [PubMed: 22323813]
50. Wolff T, Ready DF. Cell death in normal and rough eye mutants of Drosophila. Development. Nov 1991;113(3):825–39. [PubMed: 1821853]
51. Wang M, Niu W, Hu R, et al. POLR1D promotes colorectal cancer progression and predicts poor prognosis of patients. Mol Carcinog. May 2019;58(5):735–748. 10.1002/mc.22966. [PubMed: 30582221]
52. Usha N, Shashidhara LS. Interaction between Ataxin-2 Binding Protein 1 and Cubitus-interruptus during wing development in Drosophila. Dev Biol. May 15 2010;341(2):389–99. 10.1016/j.ydbio.2010.02.039. [PubMed: 20226779]
53. Neumann CJ, Cohen SM. Distinct mitogenic and cell fate specification functions of wingless in different regions of the wing. Development. Jun 1996;122(6):1781–9. [PubMed: 8674417]
54. Varadarajan S, VijayRaghavan K. scalloped functions in a regulatory loop with vestigial and wingless to pattern the Drosophila wing. Dev Genes Evol. Jan 1999;209(1):10–7. 10.1007/s004270050222. [PubMed: 9914414]
55. Wu S, Liu Y, Zheng Y, Dong J, Pan D. The TEAD/TEF family protein Scalloped mediates transcriptional output of the Hippo growth-regulatory pathway. Dev Cell. Mar 2008;14(3):388–98. 10.1016/j.devcel.2008.01.007. [PubMed: 18258486]
56. Simmonds AJ, Liu X, Soanes KH, Krause HM, Irvine KD, Bell JB. Molecular interactions between Vestigial and Scalloped promote wing formation in Drosophila. Genes Dev. Dec 15 1998;12(24):3815–20. 10.1101/gad.12.24.3815. [PubMed: 9869635]

57. Tortoriello G, de Celis JF, Furia M. Linking pseudouridine synthases to growth, development and cell competition. FEBS J. Aug 2010;277(15):3249–63. 10.1111/j.1742-4658.2010.07731.x. [PubMed: 20608977]
58. Tracey WD Jr., Ning X, Klingler M, Kramer SG, Gergen JP. Quantitative analysis of gene function in the Drosophila embryo. Genetics. Jan 2000;154(1):273–84. 10.1093/genetics/154.1.273. [PubMed: 10628987]
59. Zhang Q, Shalaby NA, Buszczak M. Changes in rRNA transcription influence proliferation and cell fate within a stem cell lineage. Science. Jan 17 2014;343(6168):298–301. 10.1126/science.1246384. [PubMed: 24436420]
60. Sanchez CG, Teixeira FK, Czech B, et al. Regulation of Ribosome Biogenesis and Protein Synthesis Controls Germline Stem Cell Differentiation. Cell Stem Cell. Feb 4 2016;18(2):276–90. 10.1016/j.stem.2015.11.004. [PubMed: 26669894]
61. Banovic D, Khorramshahi O, Owald D, et al. Drosophila Neuroligin 1 Promotes Growth and Postsynaptic Differentiation at Glutamatergic Neuromuscular Junctions. Neuron. 2010;66(5):724–738. 10.1016/j.neuron.2010.05.020. [PubMed: 20547130]
62. He F, James A, Raje H, Ghaffari H, DiMario P. Deletion of Drosophila Nopp140 induces subcellular ribosomopathies. Chromosoma. Jun 2015;124(2):191–208. 10.1007/s00412-014-0490-9. [PubMed: 25384888]
63. Cenik ES, Meng X, Tang NH, et al. Maternal Ribosomes Are Sufficient for Tissue Diversification during Embryonic Development in C. elegans. Dev Cell. Mar 25 2019;48(6):811–826 e6. 10.1016/j.devcel.2019.01.019. [PubMed: 30799226]
64. Trainor PAA, Briane T. Facial Dysostoses: Etiology, Pathogenesis and Managements. Am J Med Genet C Semin Med Genet. 2013;163(4).
65. Giampietro PF, Armstrong L, Stoddard A, et al. Whole exome sequencing identifies a POLRID mutation segregating in a father and two daughters with findings of Klippel-Feil and Treacher Collins syndromes. Am J Med Genet A. Jan 2015;167A(1):95–102. 10.1002/ajmg.a.36799. [PubMed: 25348728]
66. Lu M, Yang B, Chen Z, Jiang H, Pan B. Phenotype Analysis and Genetic Study of Chinese Patients With Treacher Collins Syndrome. Cleft Palate Craniofac J. Aug 16 2021:10556656211037509. 10.1177/10556656211037509.
67. Schaefer E, Collet C, Genevieve D, et al. Autosomal recessive POLR1D mutation with decrease of TCOF1 mRNA is responsible for Treacher Collins syndrome. Genet Med. 2014;16(9):720–724. 10.1038/gim.2014.12. [PubMed: 24603435]
68. Newton CR, Graham A, Heptinstall LE, et al. Analysis of any point mutation in DNA. The amplification refractory mutation system (ARMS). Nucleic Acids Res. Apr 11 1989;17(7):2503–16. 10.1093/nar/17.7.2503. [PubMed: 2785681]
69. Little S. Amplification-refractory mutation system (ARMS) analysis of point mutations. Curr Protoc Hum Genet. May 2001;Chapter 9:Unit 9 8. 10.1002/0471142905.hg0908s07.
70. Liu Y, Cerejeira Matos R, Heino TI, Hietakangas V. PWP1 promotes nutrient-responsive expression of 5S ribosomal RNA. Biol Open. Nov 22 2018;7(11):bio037911. 10.1242/bio.037911.
71. Gabler F, Nam SZ, Till S, et al. Protein Sequence Analysis Using the MPI Bioinformatics Toolkit. Curr Protoc Bioinformatics. Dec 2020;72(1):e108. 10.1002/cpbi.108. [PubMed: 33315308]
72. Zimmermann LS A; Nam SZ; Rau D; Kübler J; Lozajic M; Gabler F; Söding J; Lupas AN; Alva V. A Completely Reimplemented MPI Bioinformatics Toolkit with a New HHpred Server at its Core. J Mol Biol. 2018;430(15):2237–2243. [PubMed: 29258817]
73. Liu H, Naismith JH. An efficient one-step site-directed deletion, insertion, single and multiple-site plasmid mutagenesis protocol. BMC Biotechnol. Dec 4 2008;8(91):91. 10.1186/1472-6750-8-91. [PubMed: 19055817]

Key Findings

1. POLR1D is required for *Drosophila* larval growth and developmental progression.
2. A conserved glycine in POLR1D is required for *Drosophila* and human development.
3. Loss of POLR1D function in *Drosophila* neural cells causes developmental defects.
4. An RNAi screen reveals a requirement for POLR1D function in the proper development of a variety of cell types
5. *Drosophila* is an attractive model to evaluate the genetic and molecular defects of TCS mutations in POLR1D.

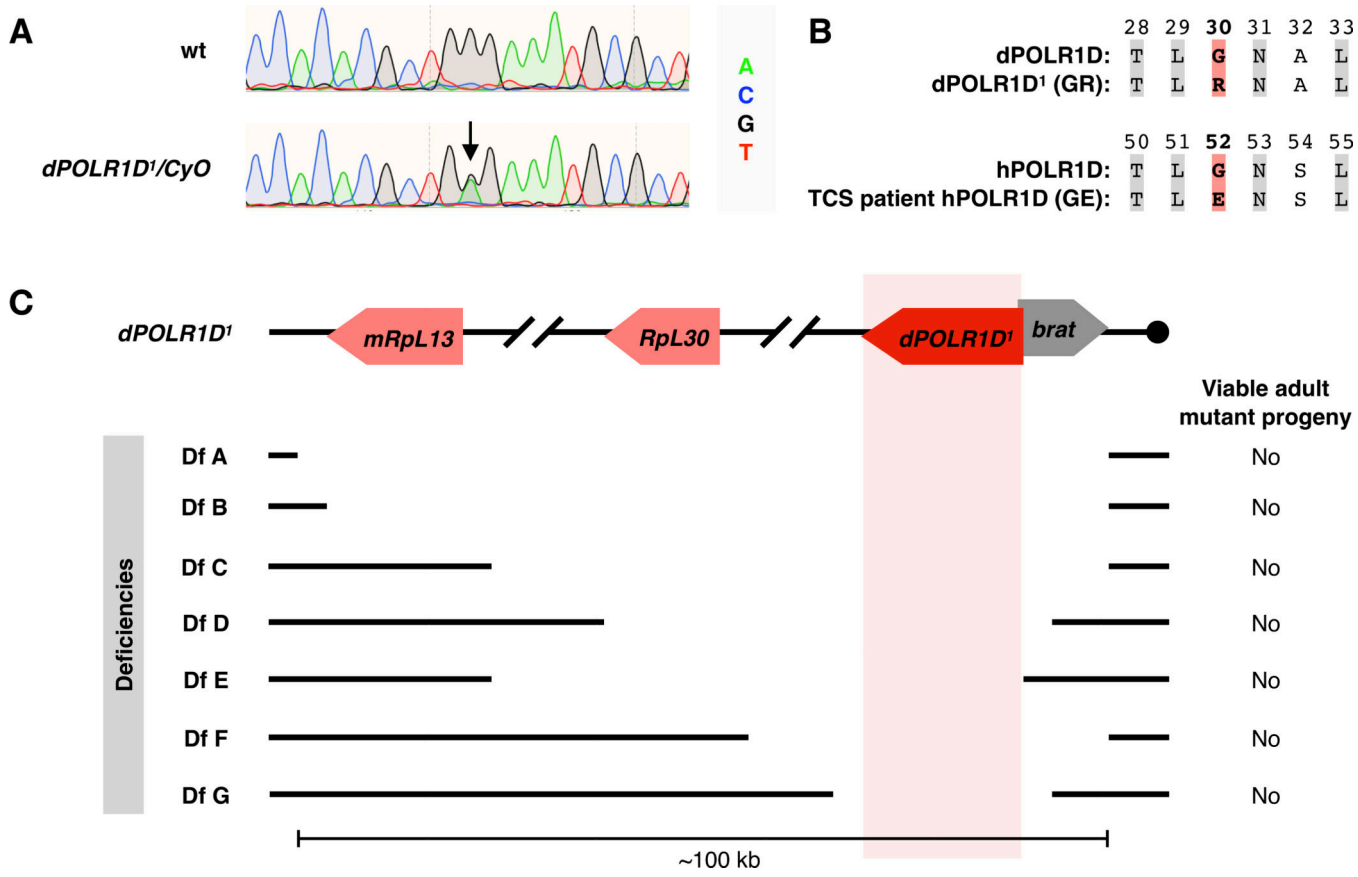

Fig. 1. The *dPOLR1D*^{1} allele is a missense mutation in a conserved glycine that causes pre-adult lethality.

(A) Chromatograms of DNA sequencing reads of the *dPOLR1D* ORF from wt and *dPOLR1D*^{1}*/CyO* male flies. A guanine to adenine transition results in missense mutation (arrow). **(B)** The missense mutation causes an amino acid substitution in a conserved glycine. This glycine is mutated to arginine in *Drosophila* and glutamic acid in a TCS patient (residues in red). Residues in grey are conserved between *Drosophila* and humans, and residues in white are not conserved. **(C)** Schematic of an ~100 kb region comprising *dPOLR1D* and adjacent genes (not to scale). The *dPOLR1D*^{1} allele is indicated. *RpL30* and *mRpL13* are upstream of *dPOLR1D* on the bottom strand; *brat* noncoding sequences overlap with *dPOLR1D* introns on the top strand. Chromosomes with regions deleted by Dfs are shown as black lines with gaps. The position of *dPOLR1D*^{1} within the deleted regions is indicated in pale red. Whether viable *dPOLR1D*^{1}*/Df* progeny from each cross were identified is indicated on the right.

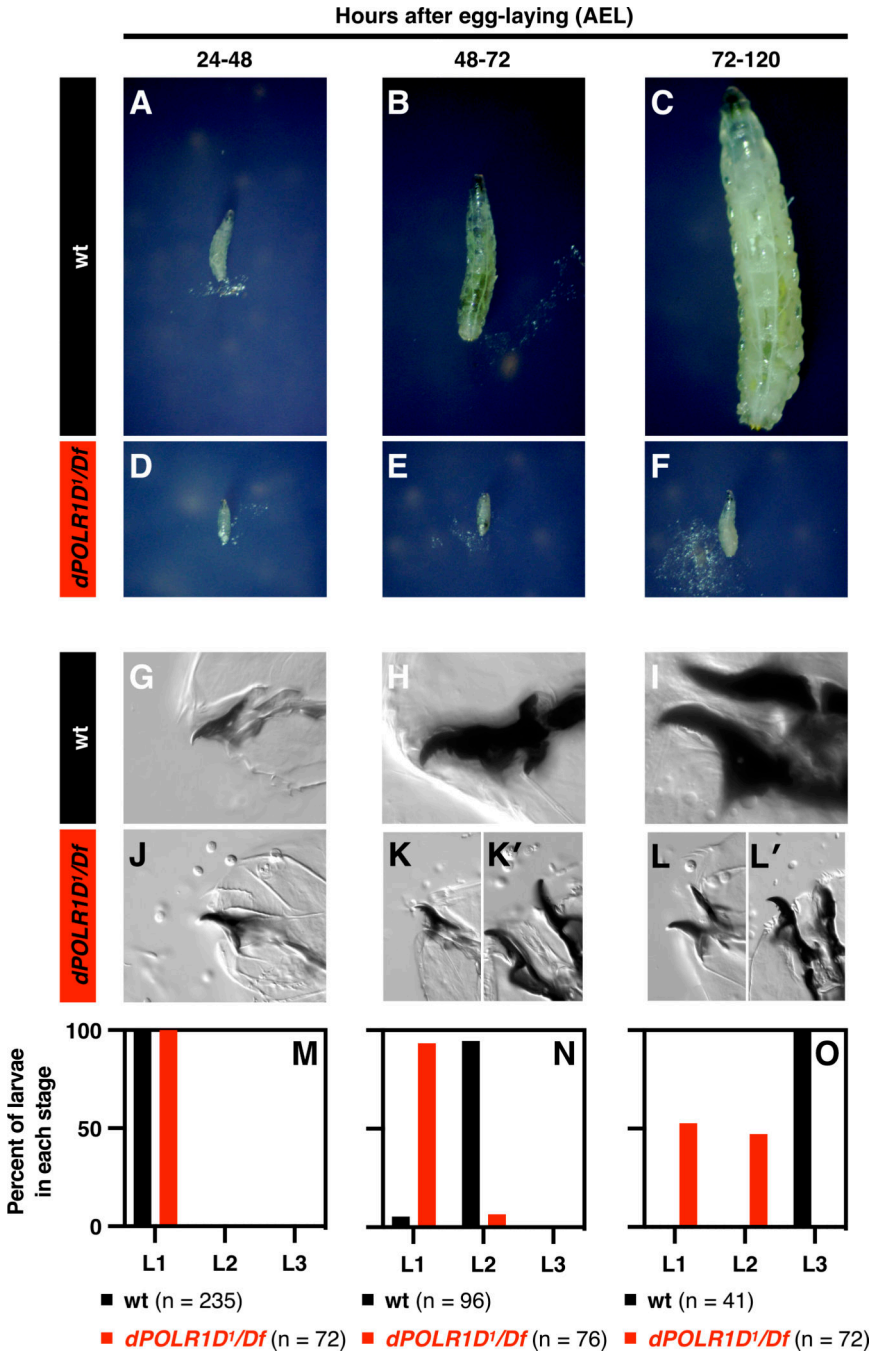

Fig. 2. *dPOLR1D^1/Df* larvae have reduced growth and are arrested in the L2 larval instar stage. wt **(A-C)** and *dPOLR1D^1/Df* **(D-F)** larvae, and cuticle preparations from wt **(G-I)** and *dPOLR1D^1/Df* **(J-L′)** larvae, at three timepoints corresponding to the L1 (24–48 h AEL), L2 (48–72 h AEL), and L3 (72–120 h AEL) stages expected in wt larvae. **K** and **K′**, and **L** and **L′** indicate L1 and L2 head skeletons of *dPOLR1D^1/Df* larvae, respectively, at the 48–72 and 72–120 h AEL timepoints. **(M-O)** Quantification of data in Figs. 2G-L′. Mouth hook morphology was scored to identify the stage of each larva. wt larvae develop as

expected, but *dPOLR1D*^{1}*/Df* larvae do not, indicating that the G30R mutation slows growth and arrests development.

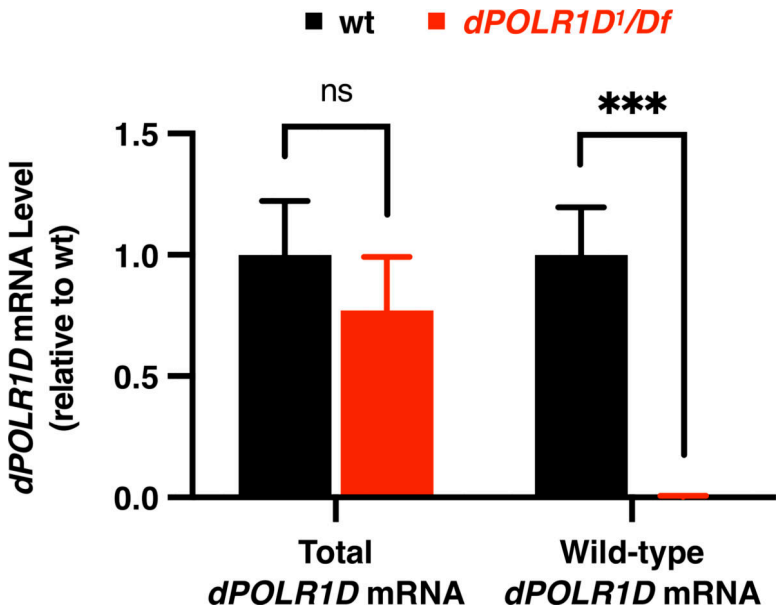

Fig. 3. *dPOLR1D*^{1} mRNA undergoes dosage compensation and is the only *dPOLR1D* allele expressed in *dPOLR1D*^{1}*/Df* larvae.

Bar graph showing the amount of *dPOLR1D* mRNA in wt and *dPOLR1D*^{1}*/Df* larvae at 72–120 h AEL, relative to wt. Total *dPOLR1D* mRNA was detected with a primer common to both the wild-type and mutant alleles of *dPOLR1D*. The wild-type allele of *dPOLR1D* was detected with an allele-specific primer. *dPOLR1D*^{1}*/Df* larvae do not accumulate any mRNA from the wild-type *dPOLR1D* allele, but there is no significant difference in the total amount of *dPOLR1D* mRNA between wt and *dPOLR1D*^{1}*/Df* larvae. Error bars represent the mean ± SEM of experiments performed in biological quadruplicate and technical triplicate. Statistical significance was calculated by ANOVA using Bio-Rad Maestro, with P-values of <0.001 (***) and not significant (ns) indicated.

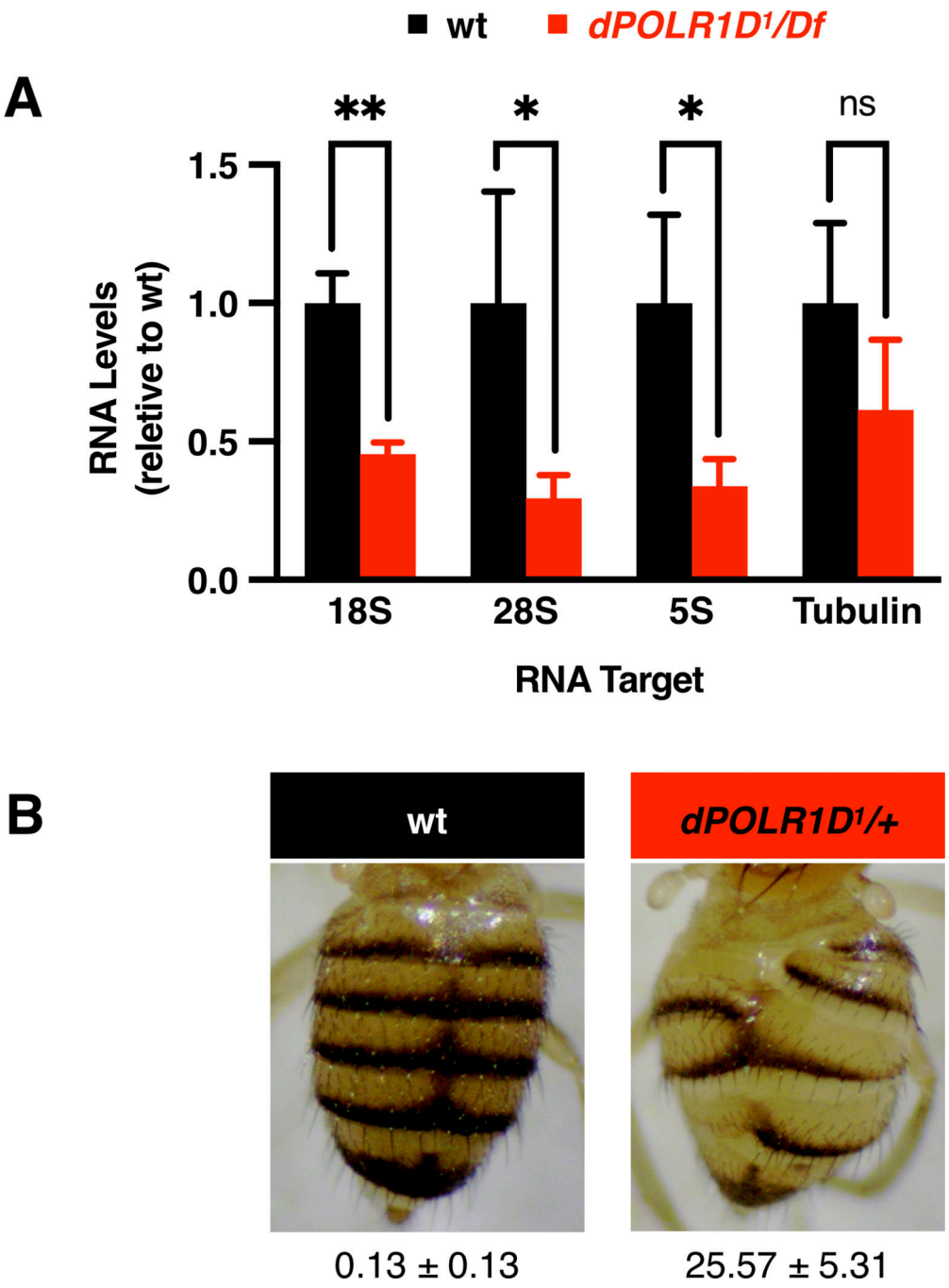

Fig. 4. The *dPOLR1D*^{1} allele affects rRNA expression.

(A) Bar graph showing the amount of rRNAs in *dPOLR1D*^{1}*/Df* larvae relative to wt larvae at 72–120 h AEL. *dPOLR1D*^{1}*/Df* larvae exhibit a significant decrease in 18S, 28S, and 5S rRNAs, but not *Tubulin* mRNA, indicating that loss of *dPOLR1D* activity affects both Pols I (18S and 28S rRNAs) and III (5S rRNA), but not Pol II (*Tubulin* mRNA). Error bars represent the mean ± SEM of experiments performed in biological quadruplicate and technical triplicate. Statistical significance was calculated by ANOVA using Bio-Rad Maestro, with P-values of <0.05 (*), <0.01 (**), and not significant (ns) indicated. **(B)**

Images of fly cuticles from the indicated genotypes. The percent of flies (± SEM) exhibiting disrupted tergites (the *bobbed* phenotype) are indicated underneath. A significant number *dPOLR1D*^{1}*/+* flies have the *bobbed* phenotype, compared to wt flies (P=0.0087). Statistical significance was calculated by two-tailed unpaired t-test using GraphPad Prism 9.3.

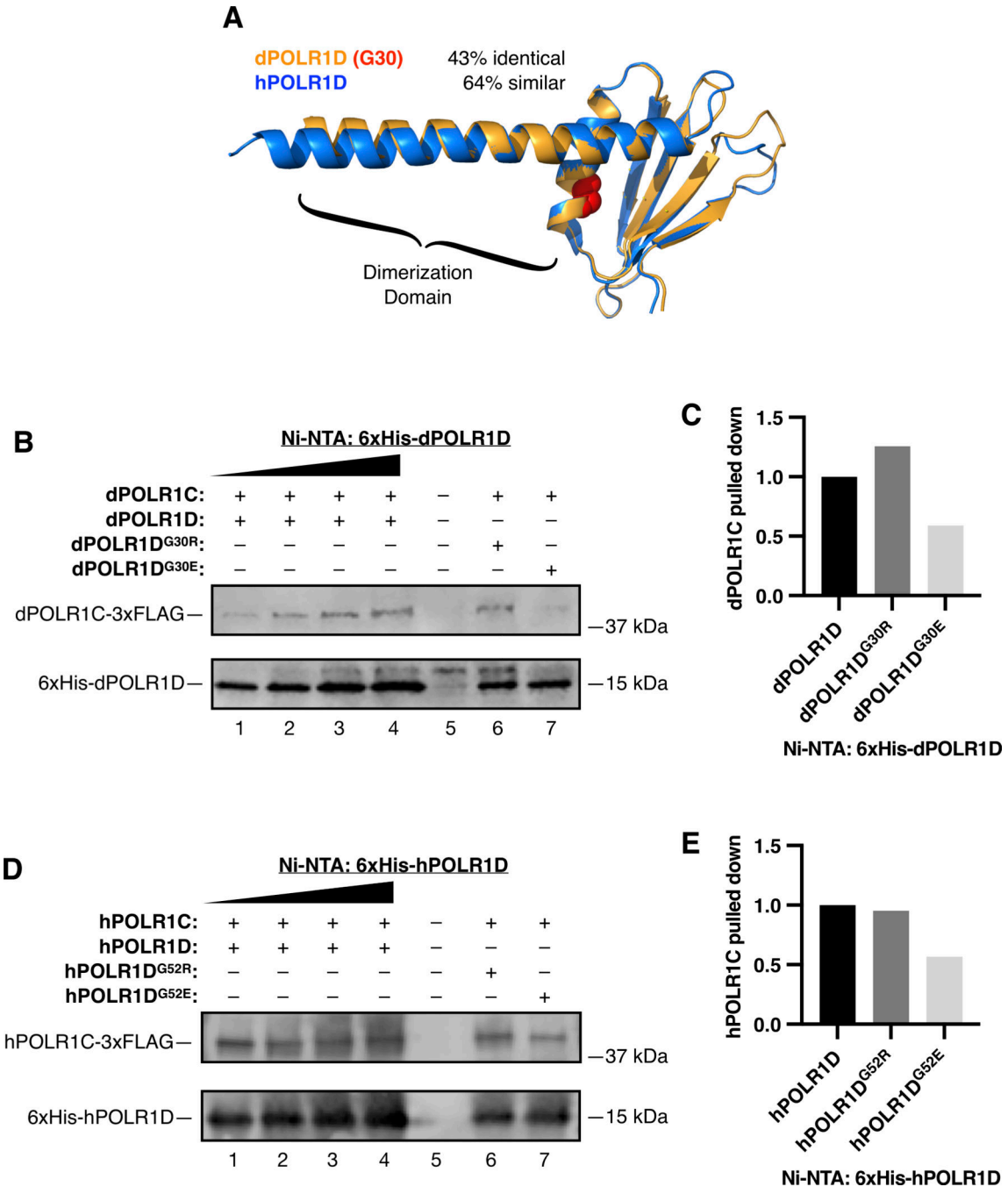

Fig. 5. *Drosophila* and human POLR1D mutations have different effects on POLR1C heterodimerzation.

(A) Overlay of dPOLR1D (orange) and hPOLR1D (blue), with the G30 residue in dPOLR1D indicated (red). dPOLR1D was modeled onto hPOLR1D (PDB 7AE1, chain K) using the HHpred MPI Bioinformatics Toolkit[71,72]. The model indicates structural conservation between dPOLR1D and hPOLR1D. **(B)** SDS-PAGE analysis of Ni-NTA purified 6xHis-dPOLR1D proteins with dPOLR1C-3xFLAG. Lanes 1–4 are a titration of a single 6xHis-dPOLR1D pulldown. **(C)** Relative quantification of the gel in (B). Lane 2

was used as the calibrator for lanes 6 and 7. **(D)** Western blot analysis of Ni-NTA purified 6xHis-hPOLR1D proteins with hPOLR1C-3xFLAG. Lanes 1–4 are a titration of a single 6xHis-hPOLR1D pulldown. **(E)** Relative quantification of the Western blot in (D). Lane 1 was used as the calibrator for lane 6, and lane 2 was used as the calibrator for lane 7. G to E mutations affect POLR1C binding, but the G to R mutations do not.

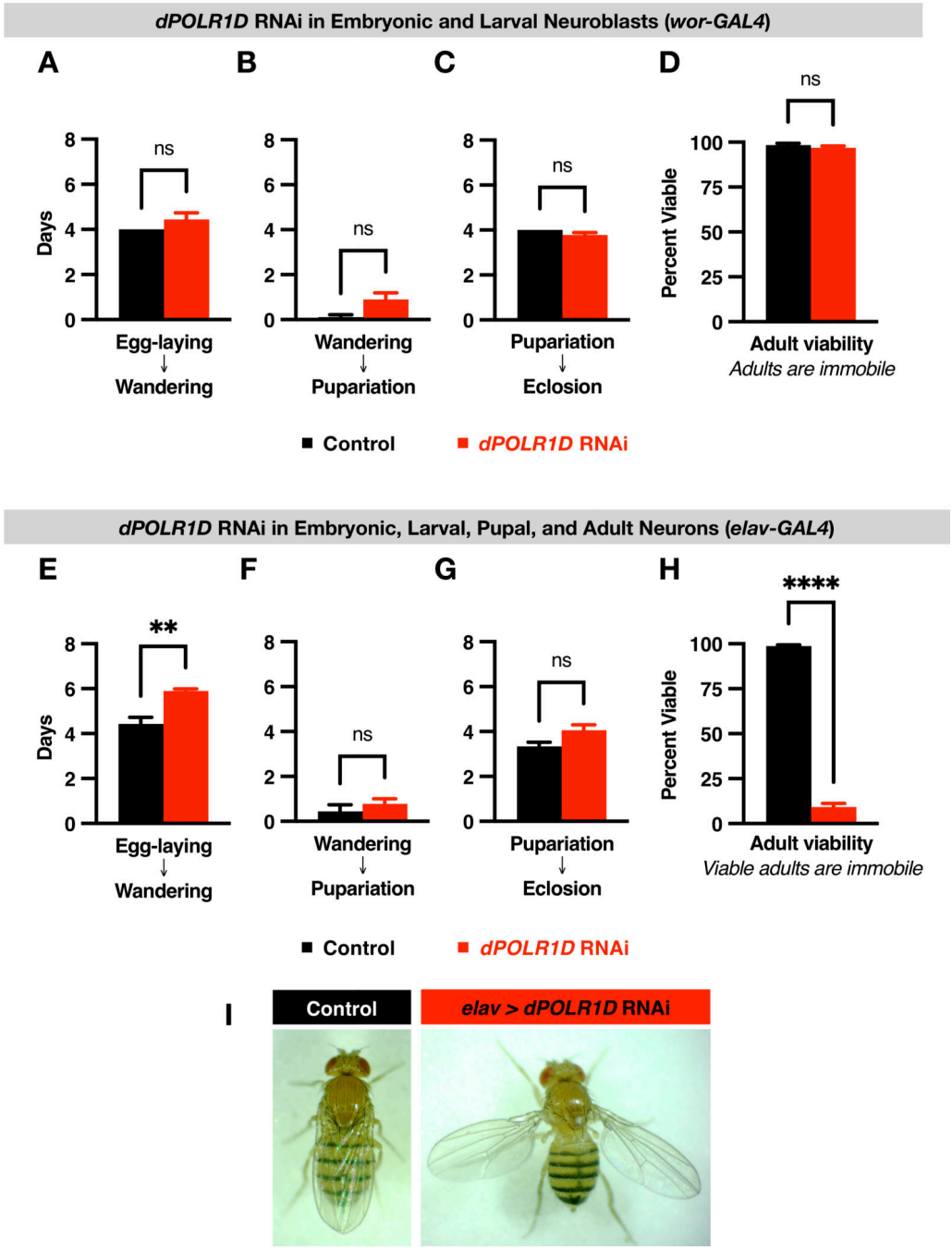

Fig. 6. dPOLR1D is required in neuroblasts and neurons for development, and adult viability and behavior.

Knockdown in embryonic and larval neuroblasts with *wor-GAL4* **(A-D)**, or pan-neuronal knockdown with *elav-GAL4* **(E-I)**. Bar graphs indicate the number of days after egg-laying it took for larvae to begin wandering **(A,E)**, the days between the onset of wandering and pupariation **(B,F)**, the days between pupariation and eclosion **(C,G)**, and the percent of viable adults **(D,H)**. Error bars represent the mean ± SEM of experiments performed in biological and technical triplicate. Statistical significance was calculated by two-tailed

unpaired t-test using GraphPad Prism 9.3, with P values of <0.01 (**), <0.0001 (****), and not significant (ns) indicated. **(I)** Images of 1–3 day-old control and *elav > dPOLR1D* RNAi adult flies. RNAi flies exhibit a *held-out wings* phenotype.

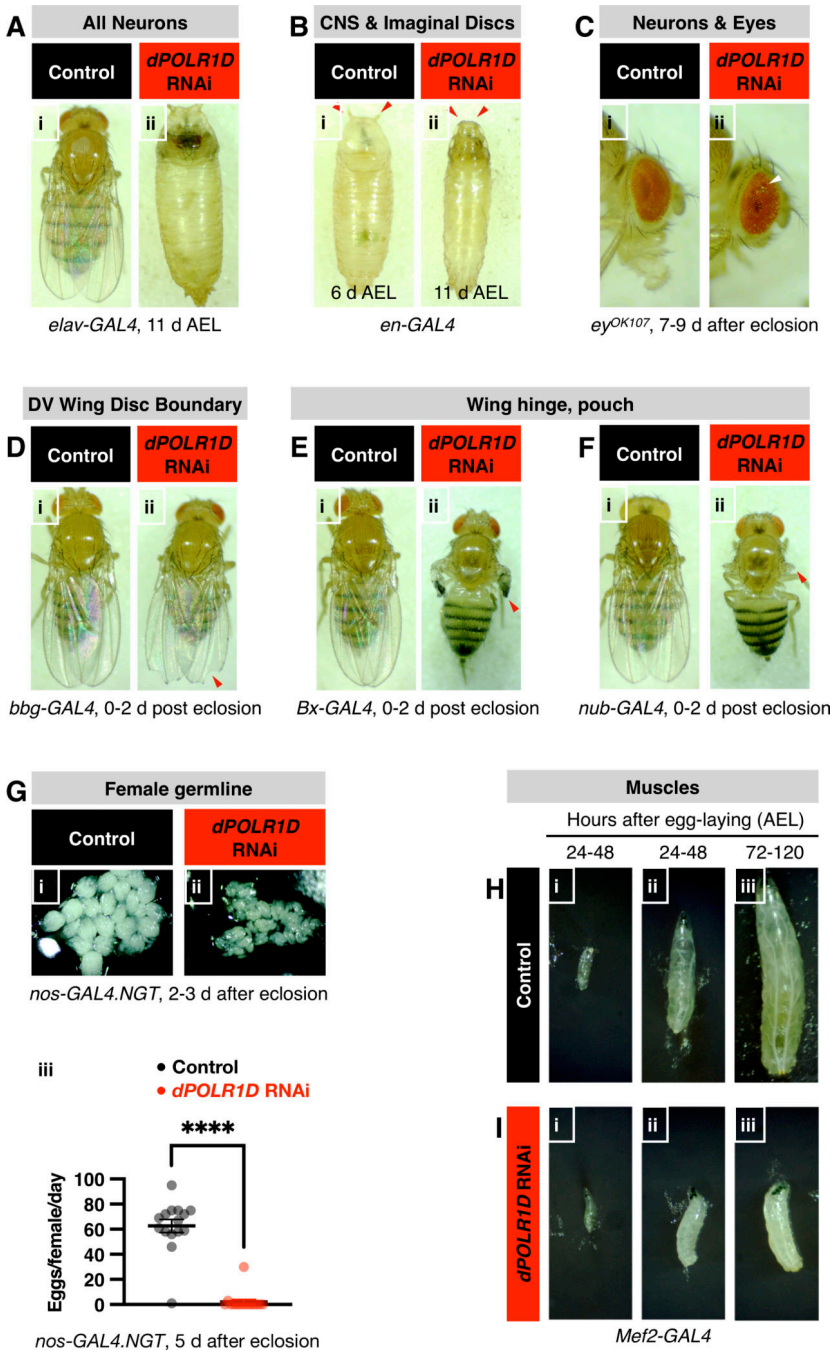

Fig. 7. Knockdown of dPOLR1D in different cell types yields developmental and functional defects.

Females harboring either an empty landing site (control) or transgenic insertion of a dsRNA targeting *dPOLR1D* (*dPOLR1D* RNAi) were crossed with males harboring the indicated GAL4 drivers and a *UAS-Dcr-2* transgene, which enhances the activity of the RNAi pathway (except in C). **(A)** Pan-neuronal knockdown with *elav-GAL4* caused pupal lethality. **(B)** Knockdown in the posterior compartments of larval imaginal discs and cells of the nervous system with *en-GAL4* caused delayed pupariation, anterior spiracle eversion

defects (red arrowheads), and pupal lethality. **(C)** Knockdown in the eye with ey^{OK107} caused a mild rough-eye phenotype (white arrowhead). **(D-F)** Knockdown with *bbg-GAL4* (dorsoventral wing disc boundary), and *Bx-GAL4* and *nub-GAL4* (wing hinge and pouch), caused wing morphology defects (red arrowheads). **(G)** Knockdown in female germline with *nosGAL4.NGT* reduced ovary size and fertility. Error bars represent the mean ± SD of cumulative data from experiments performed in biological triplicate. Statistical significance was calculated by two-tailed unpaired t-test using GraphPad Prism 9.3, with a P value of <0.0001 (****) indicated. **(H,I)** Knockdown in muscle with *Mef2-GAL4* caused arrested development.

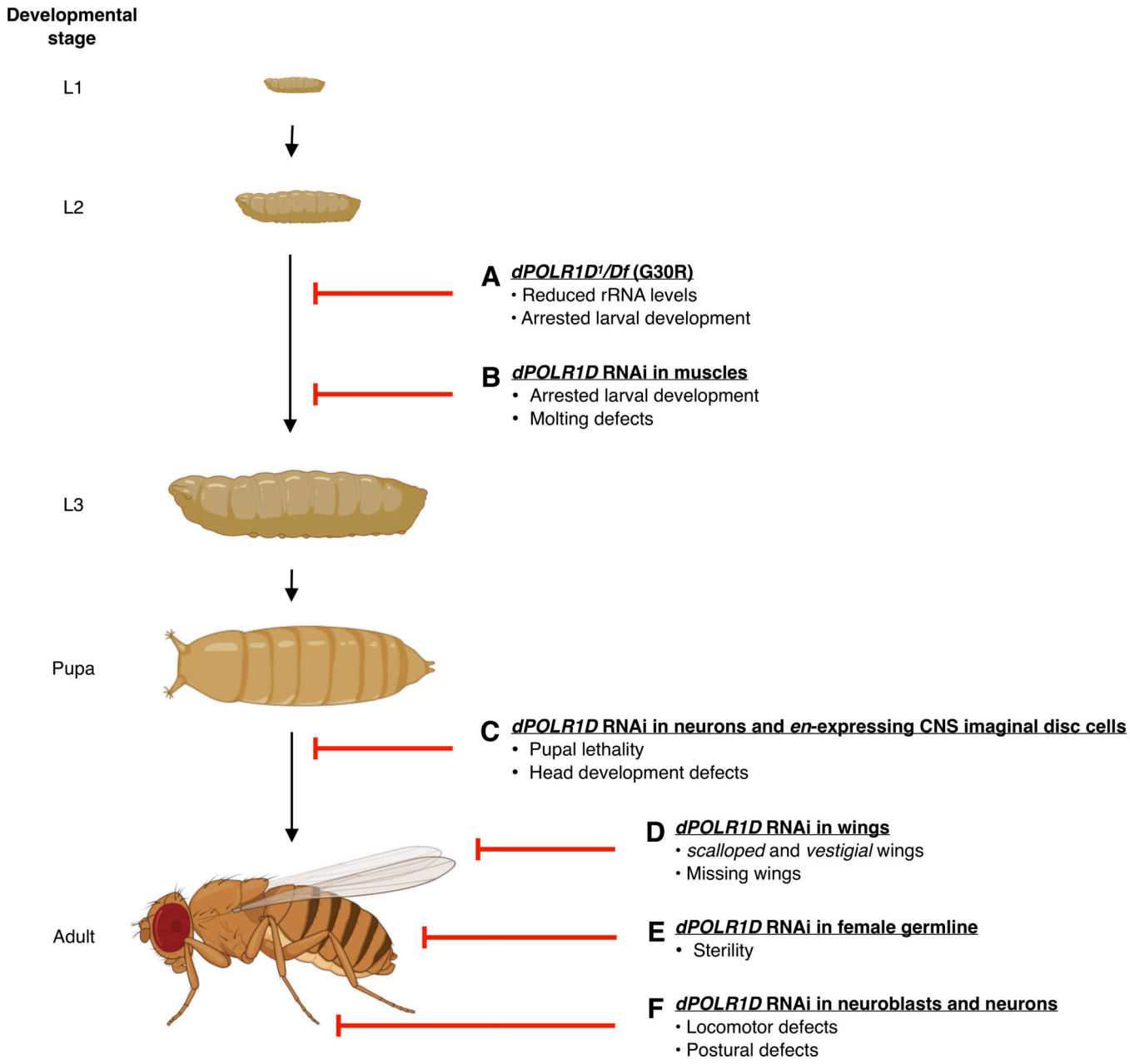

Fig. 8. Model of dPOLR1D function in *Drosophila* development.

Illustration indicating the sequential development of *Drosophila* from L1 larvae to adult; created with BioRender.com. **(A)** The *dPOLR1D*^{1} allele, a G to R amino acid substitution, in *trans* to a Df uncovering *dPOLR1D*, causes larvae to arrest development as late as the L2 stage, coincident with reduced rRNA levels, suggesting that a sufficient amount of rRNA is required to proceed further into development. Reduced RNA levels might be due to decreased integrity of Pol I and III complexes. **(B)** *dPOLR1D* knockdown in *Mef2*-expressing cells of the CNS and/or muscles also leads to developmental arrest at the L2 stage. **(C)** Pan-neuronal knockdown of *dPOLR1D* causes pupal lethality, with some adult escapers that have a *held-out wings* phenotype. *dPOLR1D* knockdown in *en*-expressing cells

of the CNS and imaginal discs leads to failure of anterior spiracles to evert, and pupal lethality. **(D)** *dPOLR1D* knockdown in the wing leads to defects in wing morphology. **(E)** *dPOLR1D* knockdown in female germline severely compromises the morphology of ovaries, and results in complete sterility. **(F)** *dPOLR1D* knockdown in neuroblasts or all neurons yields adults that have severe locomotor and postural defects.

Table 1.

The *dPOLR1D*^{1} allele is pre-adult lethal.

Table showing the raw data from Chi-Square tests performed on crosses indicated in Fig. 1. P-values were determined for cumulative data of three independent crosses. No straight wing progeny were recovered in crosses to any Dfs, including those only uncovering *dPOLR1D*, indicating that *dPOLR1D*^{1} hemizygosity alone is pre-adult lethal.

dPOLR1D1 crossed to:	Df name	Wing Phenotype	Genotype	Expected	Observed	P-Value
wt (+/+)		Straight	*dPOLR1D1/+*	230	238	0.46
		Curly	*+/CyO*	246	238	
Df/CyO A	ED1203	Straight	*dPOLR1D1/Df*	95	0	7.56 × 10–33
		Curly	*dPOLR1D-/CyO*	190	285	
Df/CyO B	ED1202	Straight	*dPOLR1D1/Df*	89	0	9.04 × 10–31
		Curly	*dPOLR1D-/CyO*	177	266	
Df/CyO C	ED1226	Straight	*dPOLR1D1/Df*	118	0	1.70 × 10–40
		Curly	*dPOLR1D-/CyO*	237	355	
Df/CyO D	ED1200	Straight	*dPOLR1D1/Df*	70	0	1.22 × 10–24
		Curly	*dPOLR1D-/CyO*	140	210	
Df/CyO E	Exel6042	Straight	*dPOLR1D1/Df*	107	0	6.84 × 10–37
		Curly	*dPOLR1D-/CyO*	215	322	
Df/CyO F	BSC313	Straight	*dPOLR1D1/Df*	84	0	3.07 × 10–29
		Curly	*dPOLR1D-/CyO*	168	252	
Df/CyO G	Exel8040	Straight	*dPOLR1D1/Df*	100	0	2.23 × 10–34
		Curly	*dPOLR1D-/CyO*	199	299	